International Journal of Crashworthiness
Publication details, including instructions for authors and subscription information:
http://www.tandfonline.com/loi/tcrs20

Parametric study for head injury criteria response of three-year olds in a child restraint system in oblique and lateral intrusive side impact

S. Shasthri[ab], V. Kausalyah[c], Qasim H. Shah[a], K.A. Abdullah[a], M.M. Idres[a] & S.V. Wong[d]

[a] Department of Mechanical Engineering, Faculty of Engineering, International Islamic University Malaysia, Kuala Lumpur, Malaysia

[b] Mechanical Division, Faculty of Engineering, Universiti Selangor, Selangor, Malaysia

[c] Faculty of Mechanical Engineering, Universiti Teknologi MARA, Selangor, Malaysia

[d] Malaysian Institute of Road Safety Research (MIROS), Selangor, Malaysia

Published online: 30 Jul 2014.

International Journal of Crashworthiness, 2014
http://dx.doi.org/10.1080/13588265.2014.942501

Taylor & Francis
Taylor & Francis Group

Parametric study for head injury criteria response of three-year olds in a child restraint system in oblique and lateral intrusive side impact

S. Shasthri[a,b]*, V. Kausalyah[c], Qasim H. Shah[a], K.A. Abdullah[a], M.M. Idres[a] and S.V. Wong[d]

[a]*Department of Mechanical Engineering, Faculty of Engineering, International Islamic University Malaysia, Kuala Lumpur, Malaysia;* [b]*Mechanical Division, Faculty of Engineering, Universiti Selangor, Selangor, Malaysia;* [c]*Faculty of Mechanical Engineering, Universiti Teknologi MARA, Selangor, Malaysia;* [d]*Malaysian Institute of Road Safety Research (MIROS), Selangor, Malaysia*

(*Received 6 February 2014; accepted 4 July 2014*)

A parametric study is undertaken to ascertain the sensitivity of the child restraint system (CRS) design, with respect to oblique side impact at standard velocities in consideration of intrusion. A hybrid model is constructed using a combination of both finite elements and multi-body ellipsoids where a three-year-old Hybrid III child dummy is placed inside a CRS and restrained with a harness system. A prescribed structural motion simulation of a side-impact crash is carried out based on experimental data. Validation is performed and the model is shown to be acceptable for common standard injury responses as well as being greatly economical in terms of computational processing time. A plan of experiments is prepared based on the Latin hypercube sampling for six parameters involving two different crash velocities. The head injury criterion (HIC) is considered as the response in this study. The model is adapted for intrusion and oblique impact. Response surface models are shown to be suitable for the mathematical modelling of the problem and Student's *t*-test is used to assess the parameter sensitivity both qualitatively and quantitatively. Most of the parameters are seen to have greater significance for wider principle direction of force (PDOF) angles above 60°. In general, a gradual decrease in significance is observed for parameters with increasing impact velocity, with the notable exception of the impact angle. The impact angle is shown to most notably affect the HIC especially from PDOF angles 45°−75°, identified as the critical impact angle range. The far side shoulder harness slack parameter is also found to be significant in reducing the HIC.

Keywords: child restraint system (CRS); side-impact crash; head injury criterion (HIC); parametric study

1. Introduction

Child passenger injuries due to car collisions are gaining increased attention from consumers, the industry, the research community and governments. This is due to concerns whereby motor vehicle crashes have become the leading cause of death for children in many developed countries [17,24]. This has naturally led to extensive studies on the safety of child passengers. Literature has shown that child anatomy and physiology [11,26,32] necessitates a separate restraints system to be implemented during vehicle travel. Thus child restraint systems or CRSs were developed and have been documented under various circumstances to successfully mitigate child injury and death [4,20].

Although it is well known that approximately twice as many crashes with a child fatality are frontal compared to lateral, later findings show that side impacts are nearly twice as likely to result in a child fatality as frontal impacts, regardless of restraint status or seating position [7,23]. While most child restraints provide good protection in frontal impacts when used properly, side-impact testing was not mandated and has not been a main design feature for most car seats and boosters. Although recently, proposals have been made to include side-impact testing for CRS in the Federal Motor Vehicle Safety Standards (FMVSS), these are far from exhaustive [29].

The side-impact crash mode is shown to be a particularly harmful mode especially for children positioned in the rear struck side [2,23]. A study of the injury mechanism and severity indicates multiple injuries located in the head, neck, limbs and thorax region. However, more than 80% of fatalities to toddlers occurred due to head trauma [22]. In the United States, for children aged five and below, head injuries are the leading cause of death for side-impact vehicle crashes [2].

A number of factors contribute to these statistics. Chouinard et. al (2005) pointed out that unsuitable restraints, classified as CRS misuse, play a major role [8]. Of these, the presence of shoulder harness slack is noted to be a major contributing factor [9]. A study by Weber reported 80% of CRS restraint misuse in North America [31]. Among misuse of securing child occupant, 60.3% are associated with shoulder harness slack [19].

The kinematics of side-impact crash depends upon both the magnitude of the impulse from the bullet vehicle as well as its principle direction of force (PDOF)

*Corresponding author. Email: shasthri@unisel.edu.my

impacting angle. Considering the data analysis reported by Anderson, oblique crashes with PDOF 60°−90° account for 75% of all side-impact crashes [1]. Of these, 63% and 70% resulted in MAIS2+ and MAIS3+ injuries (MAIS, maximum abbreviated injury scale). Fourteen percentage of the crashes involved PDOF between angles 30° and 60° of which 35% and 27% of them resulted in MAIS2+ and MAIS3+ injuries, respectively [1]. Most common PDOF is shown to be between 60° and 75° [1,15].

In addition, Howard and Arbogast have shown that head contact with intruding door due to the bullet vehicle is a serious concern in addressing any mitigation efforts [5,13]. Literature shows that most of the higher injury severity cases recorded are due to the effect of intrusion [3,6]. The most common intrusion distance involving the rear door is reported to be between 210 and 290 mm while extreme intrusions resulting in fatalities have been reported with values of 570−620 mm [1]. The general maximum intrusion depth accepted by the Economic Commission for Europe (ECE) regulation is between 170 and 280 mm with the former value associated more to newer cars [10].

Despite these data, most of the research in CRS side-impact safety does not sufficiently address these issues. The effects and relationships between the singular and cross interactive parameters with respect to the injury response are not studied. This is especially so with respect to oblique side impact involving intrusion [5]. Reliable and realistic procedures are necessary to obtain useful insights for promoting better understanding of the side-impact crash event in order to achieve greater injury mitigation.

In this work, a parametric study is undertaken to ascertain the sensitivity of the CRS design with respect to oblique side impact at standard velocities in consideration of intrusion. Numerical and statistical modelling are relatively inexpensive and efficient tools in this regard. The methodology can be seen as comprising two parts. The first part pertains to the numerical model development and validation of the crash simulation. A hybrid model is constructed using a combination of both finite elements (FE) and multi-body ellipsoids where a three-year-old child dummy model is placed inside a CRS and restrained with a harness system. A prescribed structural motion (PSM) simulation of a side-impact crash is carried out based on experimental data. Upon satisfactory validation, a plan of experiments is prepared based on the Latin hypercube sampling for six parameters involving two different crash velocities. The second part of the methodology comprises statistical model building based on regression analysis. The response surface method (RSM) is used where the head injury criterion (HIC) is defined as the response for this model. The diagnostic statistics from the regression analysis is used to assess model fitness as well as to draw conclusions on the parameter sensitivity both quantitatively and qualitatively.

2. Methods and materials

2.1. Baseline numerical model development

Data from the National Highway Traffic Safety Administration (NHTSA) of a side-impact dynamic sled test experiment (test no 4585) are adopted to serve as baseline for the model building and subsequent validation efforts [18]. In this test, a Hybrid III 3YO dummy anthropometric test device (ATD) is restrained in a forward-facing CRS. The test is conducted using the FMVSS 213 seat fixture oriented at 90° relative to the motion of the sled buck. A lateral side impact is carried out at a closing speed of 24.1 km/h (15 mph) and the acceleration pulse (pulse no TRC327) recorded is shown in Figure 1. This pulse is selected for use in this study as the loading condition in the simulation because it represents a standardised method in assessing the kinematics of the CRS and dummy during low speed (24.1 km/h), lateral side-impact crash [18]. Besides that, this test is chosen as reference as baseline model due to its freely available complete data, which is necessary for simulation model development and validation purposes. In this test, there is no rigid wall representing the surface of the interior. However, in the advanced notice proposal of rulemaking (ANPRM), the NHTSA has been considering a test that would limit head excursion such that no portion of the head of the dummy could pass through a vertical plane [16]. This plane or rigid wall is to be parallel to the longitudinal plane of the test seat assembly, and measured relative to the centreline of the CRS anchorage bar that is furthest from the simulated impact (Point Z1). This approach has been adopted in this study. A side rigid wall (height 762 mm, breadth 810 mm) is positioned 508 mm from Point Z1 as per the ANPRM specifications [16].

The numerical model developed for the simulation study is shown in Figure 2. An ellipsoid Hybrid III 3YO child dummy model is used in this study. Studies have established that the use of ellipsoid dummy models

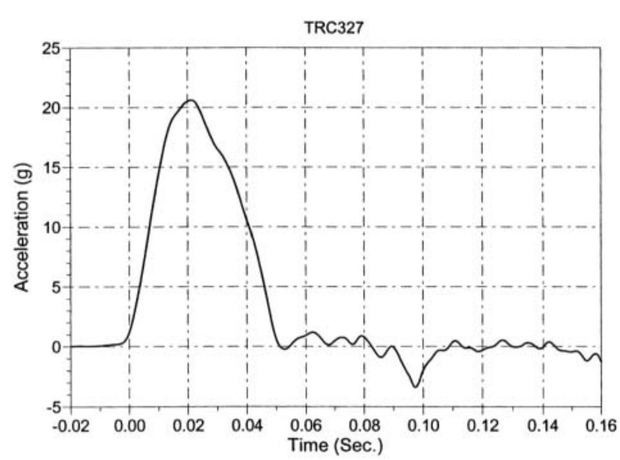

Figure 1. Pulse TRC327 − closing speed of 24.1 km/h.

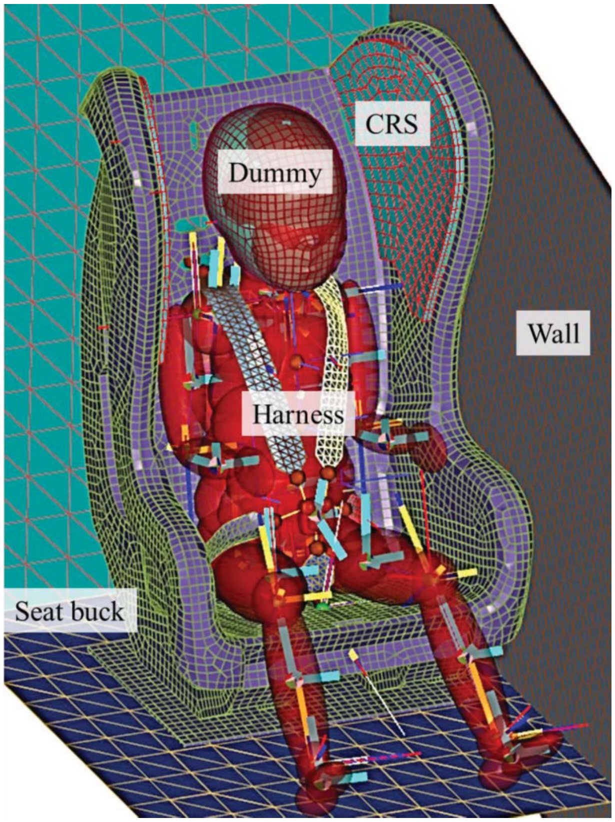

Figure 2. PSM numerical model.

drastically reduces computation time while preserving acceptable accuracy for kinematic response [25,28]. The model comprises 28 ellipsoids while certain regions of the head are built using FE. It has been developed and extensively validated by TASS International [28]. The limitations of the dummy are discussed under Section 4.1.

The R44-standard compliant CRS is modelled using shell elements with a specified thickness of 4 mm. The material property is defined as polypropylene. The density (ρ), Young's modulus (E) and Poisson's ratio (μ) are specified respectively as 800 kg/m^3, 0.842 GPa and 0.3, whereas the yield and the ultimate tensile strengths are set as 8.76 and 18.76 MPa, respectively [14,18,30]. A foam insert comprising solid elements is also modelled as shown in Figure 2. This is placed at the side wings of the CRS to absorb head impact. A highly compressible low-density foam material model ($\rho = 50.2$ kg/m^3, $E = 5.463$ MPa) is used [14,30]. The CRS is constrained at base anchorage points on an ECE R44 test bench using rigid fixed cross bars. Such an anchorage strategy has been shown to give similar trend of results for the head acceleration albeit of a more conservative magnitude due to greater CRS lateral rigidity [14]. It has been shown that this choice of CRS anchorage is effective at reducing neck loads by almost 30%, and it is expected that this will serve to offset the higher neck loads experienced by the Hybrid III dummy (see Section 4.1) [14].

The five-point harness system of the CRS is modelled predominantly using 1 mm thick membrane elements ($\rho = 890.6$ kg/m^3, $E = 2.068$ GPa, $\mu = 0.3$) [14,30]. However, to reduce computation time, the FE belts are connected at both ends to the anchor point using rigid bodies. Loading and unloading data with hysteresis are provided for both belt types [14,27,30]. No slack is allowed for the belt fitting as per conditions in Test 4585.

Both dummy and CRS are subjected to gravitational loading as well as acceleration pulse TRC327 to simulate lateral side impact. Dynamic simulation time is set to terminate after 125 ms. Convergence study is carried out during the trial runs and a good trade-off between model cost and accuracy is achieved with an element count of 24,320. All simulations are performed using MADYMO 7.4.1 by TASS on a Lenovo Thinkpad T430 (Intel 2.9 GHz quad core processor, 16 GB RAM).

2.2. *Numerical model validation*

The Hybrid model simulation results are benchmarked against experimental values and simulation results obtained by Kapoor et al. [14,18,30]. The later study involved a PSM FE simulation based on the same experiment (Test 4585) with similar boundary conditions and properties. This simulation was reported to have taken about 16 h, run from a dual core 2.6 GHz AMD Athlon processor with 2 GB of RAM. A full vehicle analysis would typically take many times that amount of time. In contrast, the computation time to run the analysis in this study using the Hybrid model took only 20 min. Despite the differences in computer systems used in the two simulations, a general conclusion may be reasonably drawn that the method presented here is able to save considerably more processing time. Furthermore, the body-segment acceleration, force and moment plots depicted in Figure 3 show that an overall good match is obtained between the experimental values and the results obtained in this study.

2.3. *Oblique impact and intrusion effect*

To study the effect of angular direction of bullet vehicle impact, the lateral pulse direction is rotated towards the bullet vehicle's principle direction of force (PDOF) lead angle φ. Figure 4 depicts a schematic diagram of the struck vehicle and the bullet vehicle, where **R** is the orientated initial pulse data set. **R** is then separated into its axial components where $\mathbf{X} = \mathbf{R} \sin \phi$ and $\mathbf{Z} = \mathbf{R} \cos \phi$. Thus a two-dimensional pulse data set which includes the lateral component **X** as well as the forward component **Z** is created. By asserting both these pulse loads upon the CRS

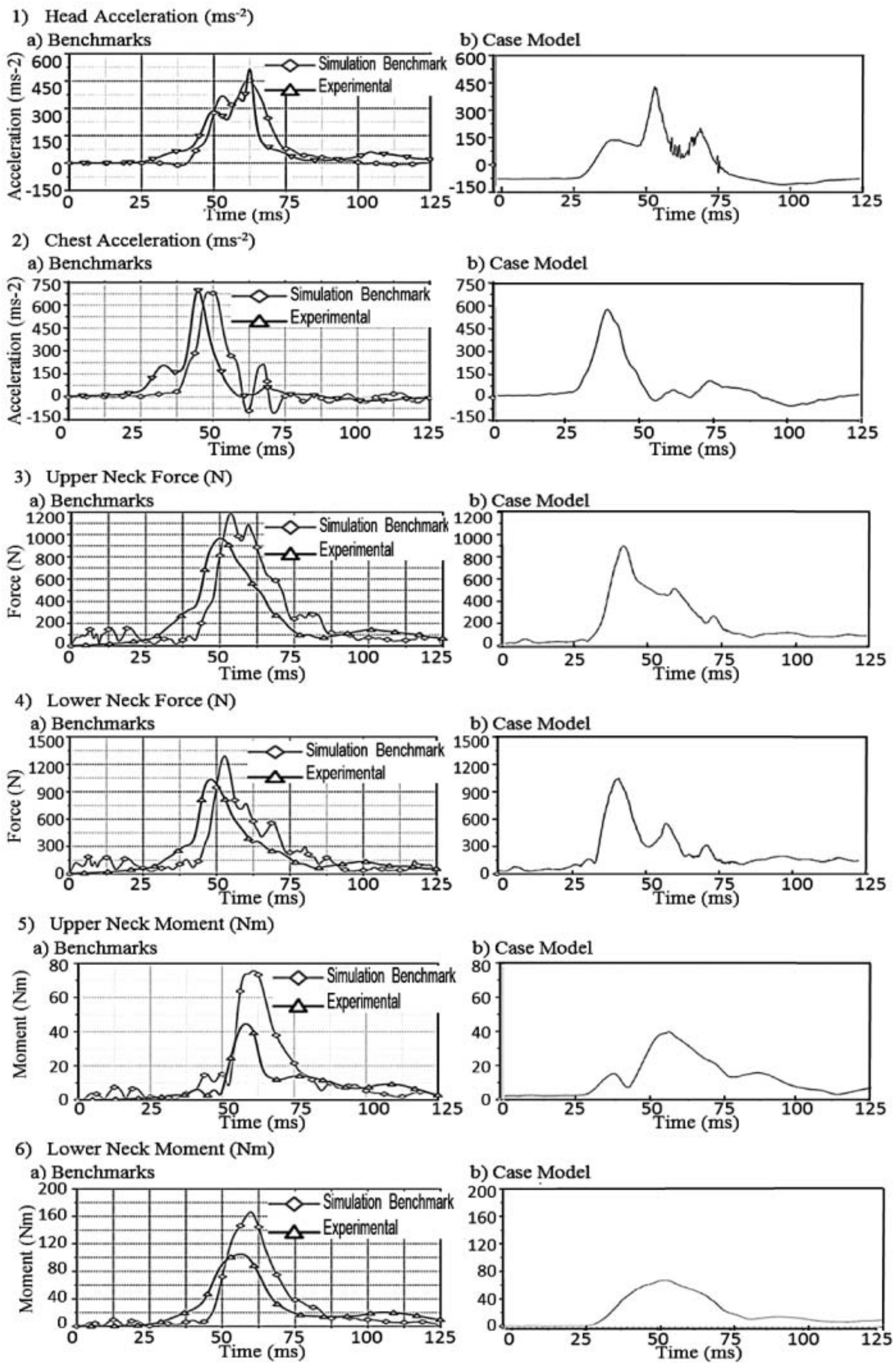

Figure 3. A comparison of body-segment response vs. time plots against benchmarks.

and the child dummy, it is assumed that an oblique impact for a given value of ϕ can be simulated adequately.

Extreme intrusions have been reported with values of 570−620 mm [1]. These certainly result in fatalities and the conditions for mitigation are too stringent for any CRS manufacturer to comply. A more practical approach of considering moderate intrusion conditions as outlined by the ECE R95 regulation may be acceptable and is considered in this study [10,12]. An intrusion of 280 mm is defined in this study and it is achieved by means of introducing rigid static planar surfaces as shown in Figure 5. The secondary intrusion plane (130 mm intrusion) has contact defined against the CRS as well as the child dummy where else for the primary intrusion plane, only the head is allowed contact with it. This arrangement is assumed to represent the worst case scenario of the intrusion whereby the head is free to strike the hardest part of the intruding door, at the earliest moment of time.

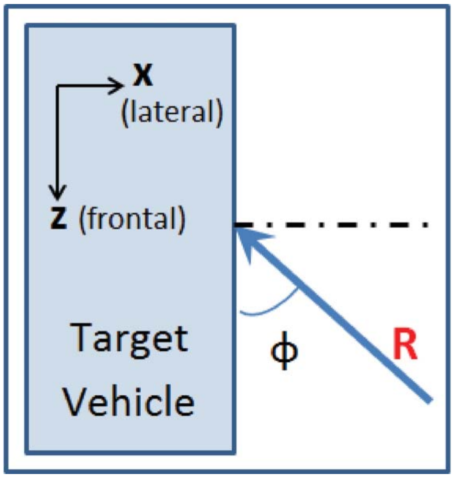

Figure 4. Schematic diagram illustrating oblique side impact on struck vehicle.

2.4. *Mathematical modelling*

Figure 6 illustrates the parameters selected for the sensitivity study. Table 1 shows organisation of the design of experiments (DoE) as well as the upper and lower bounds considered for each parameter adopted from standards [16,29]. To further increase the sensitivity of the study, the PDOF impact angle (X_1) is divided into two groups, namely PDOF A (60° ≤ ϕ ≤ 90°) and PDOF B (30° ≤ ϕ ≤ 60°). The first represents a wide PDOF angle (ϕ ≥ 60°) impact approach while the latter denotes a narrow impact approach (ϕ ≤ 60°). Two standard impact velocities, 24.1 km/h pulse TRC327 and 32.2 km/h (20 mph) pulseTRC595 (Figure 7) [12] are investigated here and therefore, each aforementioned group is further divided. Thus in total, four DoE groups are created, all of which mapping a total of 160 simulation runs. The response HIC computed from the integration of the head acceleration plots generated, are recorded.

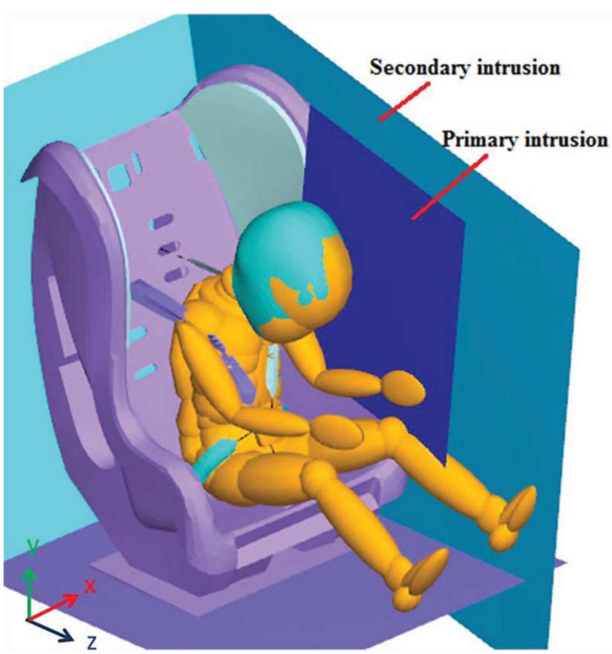

Figure 5. Oblique side-impact PSM simulation.

Multinomial regression is used as a method to determine parameter sensitivity and hence a quadratic RSM is used to model the problem. The response data are converted to logarithmic values of base 10 and submitted for regression analysis. Table 2 shows the statistical diagnostics obtained for all four models. From the regression coefficients, a good fitness is indicated for all the models. The model errors are acceptably low as indicated by the small root mean squared error (RMSE) values. The R^2 and R^2 adjusted (R^2 adj.) values substantiate this conclusion as well as provide a good indication of the model fitness with all values closely approaching unity. In addition, results from the Fisher (F) test reconfirm that the RSM models show good acceptance.

The Student's t-test is used to identify the major contributing single parameters and two-factor cross interaction parameters, as well as to assess their respective significance. The value of the single parameter or main effect is a measurement of the change in the average response as it varies from high to low levels. In the same way, the joint effects of two parameters upon a response, known as cross interaction parameters, can be measured. A positive value of the t statistic indicates that the parameter contributes to the increase of the HIC response and vice versa, while the magnitude suggests the comparative degree of that contribution. The small p values indicate the significance of the parameter contribution to the HIC. The sensitivity of the parameters individually or cross interactively with each other is ascertained in this manner for each model. This indicates the degree of sensitivity between two parameters in affecting the HIC response. The higher order quadratic terms are not considered as they are of a lesser practical interest.

3. Results

Table 3 maps the singular and cross interactive parameter sensitivity of significance for the four models, arranged according to impact angle group for the two standard impact speeds. The non-significant data are omitted, while the values of major significance are printed in bold. The complete t statistic data are presented in the form of a bar chart in Figure 8, which is useful in qualitatively analysing the behaviour pattern of each parameter with respect to HIC response in consideration of impact angle groups and impact speed. For instance, it can be seen that for parameters X_1, X_4, X_3X_6 and X_4X_5, although the relationship with the HIC response is proportional at wide impact angles (PDOF A), conversely, it becomes inversely

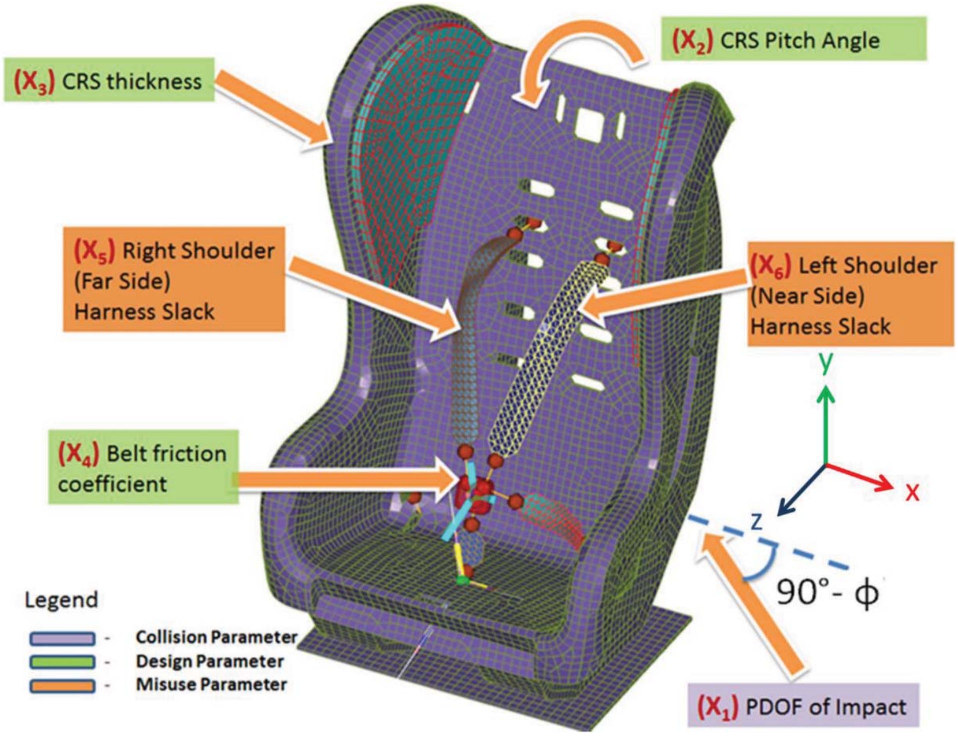

Figure 6. CRS parameters considered for oblique side impact.

proportional at narrow impact angles (PDOF B), i.e., increase in parameter decreases HIC response value.

4. Limitations

4.1. ATD dummy model

It should be noted that the Hybrid III 3YO has a shoulder and torso that are stiffer than the human child's in the lateral direction, owing to its relative rigid construct of the thoracic spine [21]. Thus there is a concern that this ATD will not fully replicate a child's kinematics in a side impact. The shoulder structure for adults and its relevance to kinematic response is not currently fully understood by the biomechanical community. However, from preliminary evaluations undertaken by the NHTSA to assess the side-impact capabilities of the Hybrid III, it is assessed that given the initial forward rotation of the dummy in a lateral test, it is possible that the shoulder would have little influence on the overall kinematic response in the side-impact tests under consideration [16]. In addition, Kapoor et al. have shown that despite variations in neck loads and chest acceleration, head acceleration values for the Hybrid III 3YO are of an acceptable range [14]. Furthermore, the choice of usage of rigid cross bar CRS anchorage is expected to offset the higher neck loads experienced by the ATD, thereby improving its biofidelic kinematic behaviour [14]. Therefore, apart from detailed injury studies pertaining to the stresses and the deformations in which the biofidelity is paramount, for a kinematic assessment such as the HIC as is the case in this study, it is deemed that the Hybrid III 3YO ATD is adequate.

Table 1. DoE grouping and parameter bounds.

Attributes	Group			
	15 PDOF A	15 PDOF B	20 PDOF A	20 PDOF B
X_1 (ϕ) (degrees)	$60° \le X_1 \le 90°$	$30° \le X_1 \le 60°$	$90° \le X_1 \le 60°$	$30° \le X_1 \le 60°$
X_2 (degrees)	$8° \le X_2 \le 24°$			
X_3 (mm)	$3.5 \le X_3 \le 5.5$			
X_4 (value)	$0.25 \le X_4 \le 0.35$			
X_5 (cm	$0 \le X_5 \le 5$			
X_6 (cm)	$0 \le X_6 \le 5$			
Pulse	24.1 km/h (TRC327)		32.2 km/h (TRC595)	

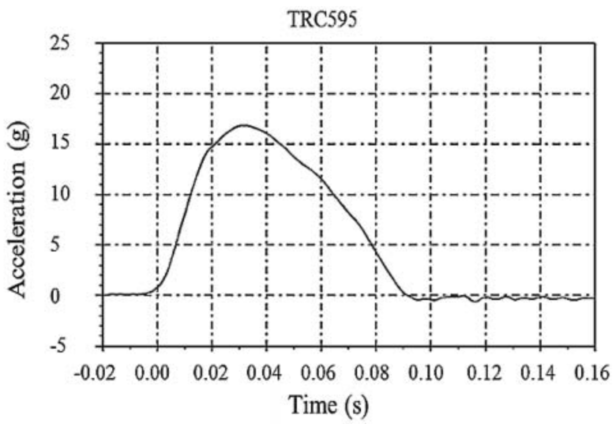

Figure 7. Pulse TRC595 – closing speed of 32.2 km/h.

Nevertheless, due to the lateral rigidity in the Hybrid III 3YO, the results are expected to be conservative.

4.2. *Oblique pulse*

In this work, due to the lack of primary data to prescribe the pulse at different impact angles, data were generated as outlined in Section 2.3. The purpose of the oblique pulse load is to create a forward (z axis) load component which is present in an oblique side impact. The pulse data used at the incremental oblique angles have a uniform y component (height). All other simulation conditions are kept identical except for the planar (x–z) pulse. Although concern may arise that such a pulse generated for oblique loading from a primary pulse may not be realistic, nevertheless, it presents a controlled uniform loading by which the results can be easily compared qualitatively. This is in line with the primary purpose of this study which is to capture the trend and significance of the various parameters at different impact angles under identical controlled loading. Thus, it can be argued, that for a preliminary study of this nature, which does not involve detailed injury assessment of tissue and bone fracture, such an assumption would not be misleading. Nevertheless, the conclusions presented here serve as a reference only as guidelines and are subject to further corroboration from experimental dynamic sled tests.

Table 2. Model fitness diagnostic statistics.

	Model fitness statistics				
	Fisher test				
RSM models	F statistic[a]	p value	R^2	R^2 adj.	RMSE
(1) 15 PDOF A	63.6787	8.5301E-19	0.9840	0.9685	0.039
(2) 20 PDOF A	68.77	2.9958E-19	0.9851	0.9708	0.048
(3) 15 PDOF B	95.6470	3.2908E-21	0.9893	0.9789	0.031
(4) 20 PDOF B	72.4183	1.4810E-19	0.9859	0.9273	0.041

[a]Where F statistic > 1.92 to satisfy null hypothesis requirement. Value of f = 1.92 is obtained from the Murdoch and Barnes table by matching regression coefficients.

5. Discussion

A cursory view of the results in Table 3 shows a higher quantitative significance of the parameters at wide impact angles ($\phi \geq 60°$) compared to narrow impact angles. Between the lower impact speed, 24.1 km/h, and the higher speed of 32.2 km/h, the latter seems to indicate a dwindling of the number of significant parameters, especially at narrow impact angles. For mitigation efforts, the results suggest that close scrutiny and optimisation of the parameters will serve to improve head injury mitigation but only when the bullet vehicle impact angle is greater than 60°. When the impact angle falls below 60°, the parameter considerations cease to have a significant effect upon the HIC. In addition, the result trends indicate that for increasing impact velocity, the parameters gradually lose their ability to influence the HIC response, all except for the PDOF impact angle (X_1). This is an important observation for it indicates that, if somehow by either active or passive measures, the effective angle of impact experienced by the child in the CRS is controlled, i.e., avoiding the critical range, it may be possible to significantly afford tangible head injury mitigation even at non-standard, elevated impact velocities.

5.1. *Primary parameter sensitivity – PDOF impact angle*

The PDOF impact angle parameter is seen to play the most prominent role in affecting the HIC response. Although, at wide impact angles ($\phi \geq 60°$), singularly by itself, it appears not to hold significance, but owing to the presence of a number of two-factor cross interaction parameters ranging from moderate (X_1X_3, X_1X_6) to high significance (X_1X_5), the PDOF impact angle seems to notably affect the HIC response indirectly. This is true for both impact speeds although the trend suggests a slight decline of significance with increasing impact velocity. At narrow impact angles, however, interestingly an opposite effect is observed. In general, the cross interaction parameters fall to relatively negligible significance, while the singular PDOF impact angle parameter stands prominent. Indeed it is seen that for higher impact speed (32.2 km/h), the PDOF impact angle parameter alone is shown to be of major importance. Contrary to wide impact angles, for narrow impact angle, i.e., $\phi \leq 60°$, the statistical data trend suggests that the parameter increases in significance with increasing impact velocity. Figure 9 shows the bell curve HIC response for the full range of X_1 values encompassing both PDOF A (wide angle) and B (narrow angle) groups. For the higher HIC values, brief whiplash-like motion of the head is seen to occur as it contacts against

Table 3. *T* test and significance *p* of parameters for HIC response.

	15 PDOF A		20 PDOF A		15 PDOF B		20 PDOF B	
Significant parameters[a]	t	p	t	p	t	p	t	p
X_1					−2.1692	0.0387	−3.3563	0.0023
X_2	2.2436	0.0329	1.7966	0.0832				
X_5	−2.3227	0.0277	−2.0708	0.0477				
X_1X_3	−2.1350	0.0416						
X_1X_5	**−3.6333**	**0.0011**	**−3.5265**	**0.0015**				
X_1X_6	−2.5287	0.0174	−2.5881	0.0151	2.0529	0.0495		
X_2X_3	−2.5733	0.0157	−2.4063	0.0230				
X_3X_4	2.1884	0.0371	1.7223	0.0960				
X_3X_5	2.2510	0.0324	2.0587	0.0489				
X_1^2	6.4208	5.94E-07	5.8536	2.72E-6	−2.1337	0.0418		
X_2^2	−3.3017	0.0026	−3.1269	0.0041	−1.7496	0.0911	−1.9765	0.0580
X_4^2	−2.0105	0.0541	−2.0520	0.0496				
X_5^2	1.7861	0.0849						

Note: Items in boldface are of high statistical significance ($p < 0.01$). The quadratic terms (X_i^2) are not considered.
[a]Only parameters having *p* value of less than 0.1 are included in the table.

the rigid primary intrusion plane. For both impact speeds, the data trends are quite similar. Some deviation in the magnitude is seen at narrow PDOF impact angles ($\phi \leq 60°$), but it is relatively small and does not seem to alter the trend. In general, i.e., irrespective of impact speed, the HIC values are noted to be high for the PDOF impact angles between 45° and 75°. This is identified as the critical PDOF impact angle range (ϕ_{cr}) and it is postulated that substantial head injury mitigation may be achieved, if by some means, this critical range is eschewed during the crash event.

5.2. *Secondary parameter sensitivity – harness slack*

Secondarily, the results indicate the shoulder harness slack misuse parameters to be a major factor in the HIC response. The high statistical significance for the cross interaction parameter with X_1 indicates that the misuse

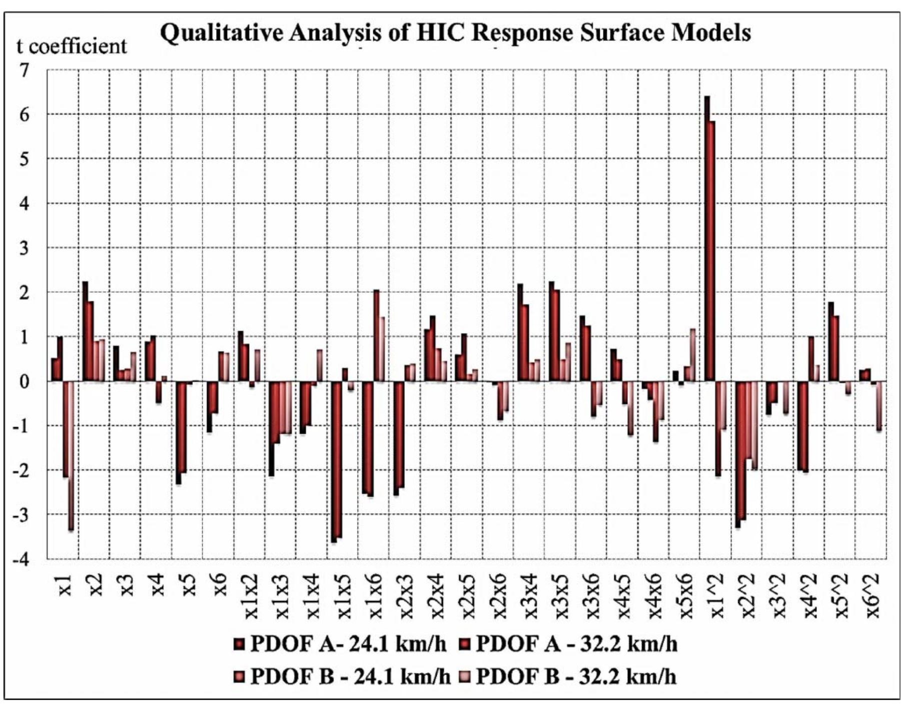

Figure 8. Qualitative analysis of HIC response for RS models.

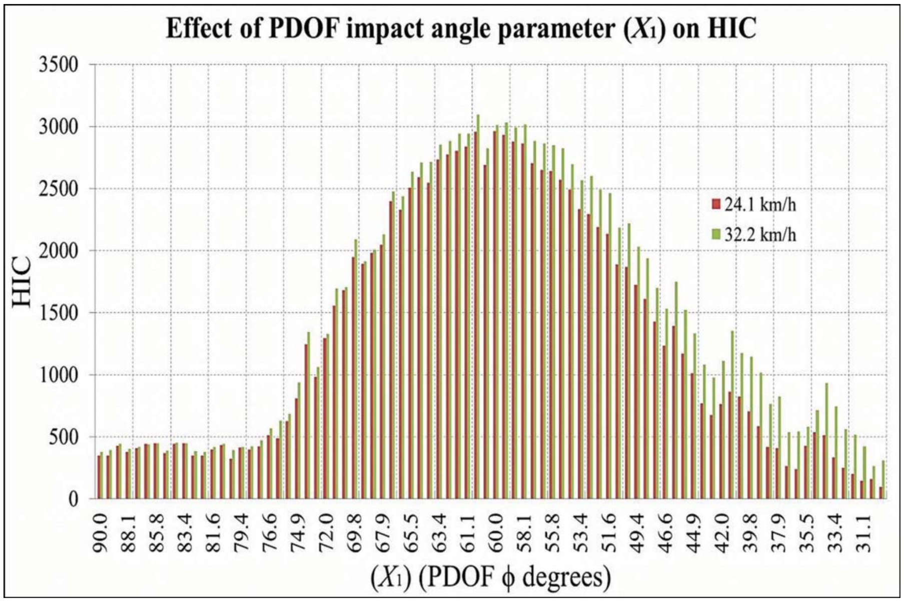

Figure 9. Effect of impact angle parameter X_1 on HIC.

parameters are highly sensitive to the direction of impact angle. First, the statistical analysis shows that between the two, the far side or right shoulder slack plays a considerably greater role in the HIC response than the near side (left shoulder). Second, it is noted that this significance is true for wide impact angles ($\phi \geq 60°$) only. Figure 10 shows the response surface plot for the X_1X_5 two-factor cross interactive parameter. It depicts the relationship between the impact angle parameter (X_1) and the right harness slack parameter (X_5) with regards to the HIC. Analysis of Table 3 as well as Figures 8 and 10, suggests that during side impact between PDOF impact angles 45° to 75° (ϕ_{cr}), the presence of slack actually proves beneficial in reducing the HIC. However, owing to the stiffness of the Hybrid III dummy's neck, this conclusion may be premature. Nevertheless, the study highlights the need for greater scrutiny in investigating this parameter effects during oblique side impact.

5.3. Nominal parameter sensitivity

As for the other parameters, at wide impact angles ($\phi \geq 60°$), a moderate significance is noted for the CRS pitch angle parameter (X_2). With regards to the HIC response, the

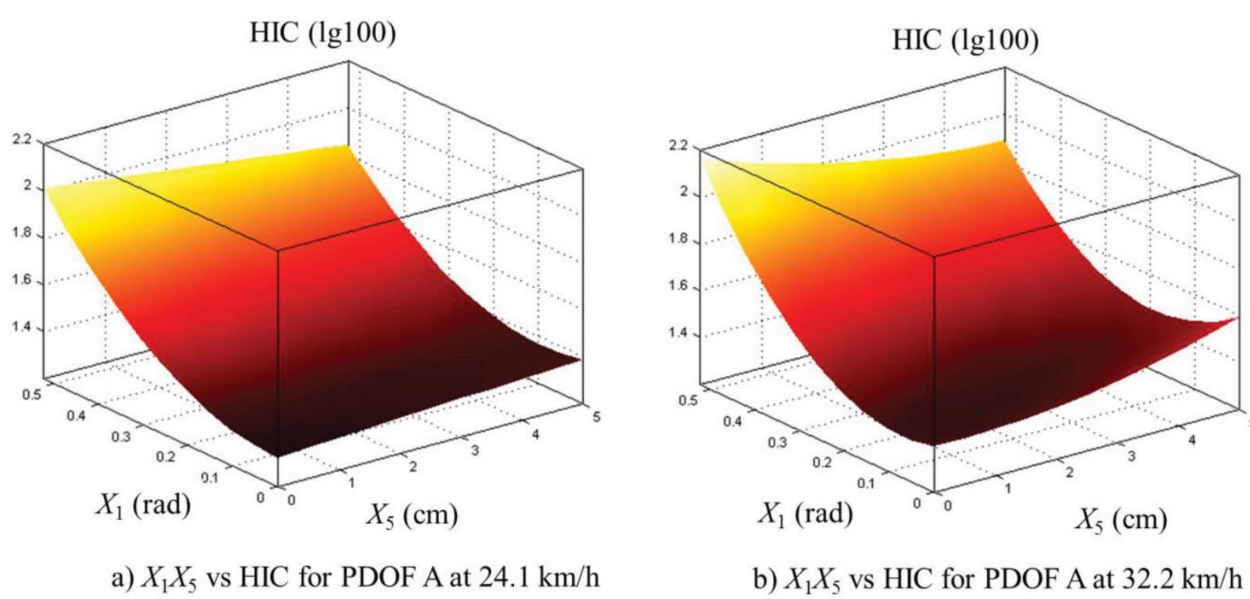

Figure 10. Response surface plot of two-factor cross interaction parameter X_1X_5.

parameter seems to be inversely proportionate to impact speed. It is also shown to be sensitive particularly to CRS shell thickness (X_3). The CRS shell thickness, on the other hand, is found to be moderately sensitive to far side harness slack (X_5) and to a lesser degree, the harness friction coefficient (X_4). Though these parameters are of only nominal significance, the observations may be of use in the consideration of an optimised CRS design towards achieving improved head protection.

6. Conclusions

A methodology is outlined in which the effect of multiple parameters on the HIC response of a three-year-old child involved in a side-impact crash is assessed. Six parameters are investigated, namely the PDOF impact angle, CRS pitch angle, CRS shell thickness, harness friction coefficient and both right and left shoulder harness slack values. The study considers the effect of intrusion and is carried out at two different impact speeds. A statistical method is used to map the sensitivity of the parameters singularly as well as cross interactively, both qualitatively and quantitatively. Notably, the findings can be summarised as follows:

(1) In general, all parameters show greater influence in affecting the HIC response at PDOF impact angles (ϕ) of 60° and above.
(2) The results trend indicates that all parameters gradually lose their ability to influence the HIC response with increasing impact velocity. The sole exception is the PDOF impact angle parameter (X_1) which in fact shows an increasing significance with increasing impact speed.
(3) The PDOF impact angle parameter (X_1) is revealed to be of primary significance.
(4) The PDOF impact angle critical range ϕ_{cr} is shown to be between impact angles 45° and 75°. Avoiding this impact angle range may result in substantial head injury mitigation.
(5) The presence of harness slack at critical impact angle range is shown to reduce HIC values. In this regard, the far side (right shoulder) slack (X_5) is shown to be statistically greater in significance than the near side or left shoulder slack (X_6).
(6) At wide PDOF impact angles ($\phi \geq 60°$), the CRS pitch angle (X_2) is shown to be moderately sensitive in affecting the HIC.

Finally, the work demonstrates a necessity for further study and experimental testing in consideration of the relationships that is parametrically shown to exist between CRS design, harness slack and PDOF impact angle of bullet vehicle with regards to HIC injury response of a three-year-old child. The findings here may serve as a useful reference in addressing head injury mitigation efforts in children during side impact. It may also serve as a reference for a more exhaustive experimental investigation, with improved side-impact ATDs, towards the development of newer test procedures and safety standards in addressing safety concerns in oblique side-impact crash.

Funding

The authors would like to acknowledge and thank the Malaysian Ministry of Higher Education (MOHE) for the awarding of a research grant [grant number FRGS 13-022-0263] in support of this work.

References

[1] M. Anderson, K. Arbogast, B. Pipkorn, and P. Lovsund, *Characteristics of crashes involving injured children in side impacts*, Int. J. Crashworthiness 16(4) (2011), pp. 365−373.
[2] K. Arbogast, I. Chen, D. Durbin, and F. Winston, *Child restraints in side impacts*, Proceedings of the International Conference on the Biokinetics of Impact, Graz, Austria, 2004.
[3] K.B Arbogast, R.A. Cornejo, M.J. Kallan, F.K. Winston, and D.R. Durbin, *Injuries to children in forward facing child restraints*, Annual Proceedings, Association of Advancement of Automotive Medicine, Vol. 46, Tempe, AZ, USA, 2002, pp. 212−230.
[4] K.B. Arbogast, D.R Durbin, R.A. Cornejo, M.J. Kallan, and F.K. Winston, *An evaluation of the effectiveness of forward facing child restraint systems*, Accident Anal. Prevention 36(4) (2004), pp. 585−589.
[5] K.B. Arbogast, G. Yoganand, R.A. Menon, S. Tylko, N. Tamborra, and R.M. Morgan, *Field investigation of child restraints in side impact crashes*, Traffic Injury Prevention 6 (2005), pp. 351−360.
[6] J. Brown, L. Bilston, M. McCaskill, and M. Henderson, *Identification of injury mechanisms for child occupants aged 2-8 in motor vehicle accidents*, Final Project Report for the Motor Accidents Authority of NSW, NSW, Paper no 07-0461, Australia, 2005. Available at: http://casr.adelaide.edu.au/rsr/RSR2006/BrownJ.pdf on Jan 2014.
[7] CHoP (Children's Hospital of Philadelphia), *Partners for child passenger safety, fact and trend report 2008*, Philadelphia, PA, 2008. Available at http://www.research.chop.edu/programs/injuries/files/PCPS_Reports/2008_FT.pdf
[8] A. Chouinard and B. Huxley, *Towards the development of a national child restraint survey*, Proceedings of Canadian Multidisciplinary Road Safety Conference XV, Fredericton, New Brunswick, June 6−9, 2005.
[9] L.E. Decina and K.Y. Knoebel, *Patterns of misuses of child safety seats*, Rep. DOT HS 808 440, National Highway Traffic Safety Administration, Washington, DC, 1996.
[10] ECE R95 − Reg 95, *Uniform provisions concerning the approval of vehicles with regard to the protection of the occupants in the event of a lateral collision*, United Nations Economic Commission for Europe, 2005. Available at http://www.unece.org/fileadmin/DAM/trans/main/wp29/wp29regs/r095a4c1e.pdf
[11] C.S. Gotschall, S. Luchter, and J.S. Wing, *Head injuries to motor vehicle occupants aged 0-5 years*, 43rd Annual

Proceedings, Association for the Advancement of Automotive Medicine, Barcelona, Spain, 1999.

[12] J. Heiko, G. Barley, S. Carine, P. Claeson, L. Bjorn, K. Nojiri, F. Renaudin, L. van Rooij, and A. Siewertsen, *Review of the development of the ISO side impact test procedure for child restraint systems*, 20th ESV Conference, Lyon, France, 2007.

[13] A. Howard, L. Rothman, and M. McKeag, *Children in side impact motor vehicle crashes: Seating position in injury mechanism*, J. Trauma 56 (2004), pp. 1276−1285.

[14] T. Kapoor, W. Altenhof, A Howard, J. Rasico, and F. Zhu, *Methods to mitigate injury to toddlers in near-side impact crashes*, Accident Anal. Prevention 40 (2008), pp. 1880−1892.

[15] L. McCray, M. Scarboro, and J. Brewer, *Injuries to children one to three years old in side impact crashes*, 20th International Technical Conference on the Enhanced Safety of Vehicles (ESV), Lyon, France, 2007.

[16] NHTSA (National Highway Traffic Safety Administration), *Advanced notice of proposed rulemaking (ANPRM)*, 49 CFR Part 571 Docket no 02-12151 RIN 2127-AI83 FMVSS 213, 2002. Available at http://www.nhtsa.gov/cars/rulings/CPSUpgrade/CPSSide/Index.htm

[17] NHTSA (National Highway Traffic Safety Administration), *Traffic safety facts 2005*, DOT HS 810 631, U.S. Department of Transportation, 2005, pp. 1−6. Available at: http://www-nrd.nhtsa.dot.gov/Pubs/810631.pdf. Accessed on Jan 2014.

[18] NHTSA (National Highway Traffic Safety Administration), *Vehicle crash test database*, Test no 4585. Available at http:www.nrd.nhtsa.dot.gov/database/aspx/vehdb/querytesttable.aspx. Accessed August 2007.

[19] Police Report/Japan Automobile Federation, *Investigation on child restraint usage (in Japanese)*, 2009. Available at http://www.jaf.or.jp/e/index_e.htm

[20] T.M. Rice and C.L. Anderson, *The effectiveness of child restraint systems for children aged 3 years or younger during motor vehicle collisions: 1996 to 2005*. Am. J. Public Health 99(2), (2009), pp. 252−257.

[21] T. Seacrist, E. Mathews, M. Samuels, J Garcia-Espana, S. Longhitano, S. St. Lawrence, S. Balasubramaniam, M. Maltese, and K. Arbogast, *Kinematic comparison of the hybrid III and Q-series pediatric ATDs to pediatric volunteers in low-speed frontal crashes*, Ann. Adv. Automotive Med. 56 (2012), 285−298.

[22] C.P. Sherwood, S.A. Ferguson, and J.R. Crandall, *Factors leading to crash fatalities to children in child restraints*, Association for the Advancement of Automotive Medicine Annual Proceedings, Lisbon, Portugal, 2003.

[23] M. Starnes and A.M Eigen, *Fatalities and injuries to 0-8 years old passenger vehicle occupants based on impact attributes*, Rep. no. DOT HS 809 410, NHTSA, Washington, DC, 2002.

[24] Statistics Canada, *Major causes of death*, Government of Canada, 2003. Available at http://142.206.72.67/02/02b/02b_003_e.htm. Accessed February 2007.

[25] M.D. Surcel and M. Gou, *Intrusion influence on child occupant behaviour in the case of a side impact MADYMO simulation*, Paper no. 05-0050, Ecole Polytechnique de Montreal, Canada, 2005.

[26] C. Tingvall, *Children in cars*. Acta Paediatrica Scand. (Suppl. 339). Thesis, ISSN 0300-8843, 1987.

[27] TNO Automotive, *MADYMO applications manual version 7.4.1*, Delft, Netherlands, 2013.

[28] TNO Automotive, *MADYMO model manual version 7.4.1*, TASS International, Delft, Netherlands, 2013.

[29] U.S. Federal Register, Vol. 79, January 28, 2014, pp. 4570−4608. Available at http://www.gpo.gov/fdsys/pkg/FR-2014-01-28/html/2014-01568.htm.

[30] Q. Wang, T. Kapoor, M.Tot, W. Altenhof, and A Howard, *Child restraint seat design considerations to mitigate injuries to three year old children in side impact crashes*, Int. J. Crashworthiness 12(6) (2007), pp. 629−644.

[31] K. Weber, *Crash protection for child passengers: A review of the best practice*, UMTRI Res. Rev. 31(3) 2000, pp. 1−28. Available at http://www.umtri.umich.edu/library/pdf/webe.pdf

[32] N. Yoganandan, S. Kumareson, F.A. Pintar, and T.A. Gennarelli, *Biomechanical tolerance criteria for paediatric populations*, AAAM-IRCOBI Child Occupant Protection, Professional Engineering Publishing, London, England, 1999, pp. 97−112.